Signals for low scale gravity in the process $\gamma\gamma \rightarrow ZZ$

Micheal S. Berger* and Brandon Zerbe†

Physics Department, Indiana University, Bloomington, Indiana 47405, USA
(Received 6 August 2005; published 11 November 2005)

We investigate the sensitivity of future photon-photon colliders to low scale gravity scenarios via the process $\gamma\gamma \rightarrow ZZ$ where the Kaluza-Klein boson exchange contributes only when the initial state photons have opposite helicity. We contrast this with the situation for the process $\gamma\gamma \rightarrow \gamma\gamma$ where the t and u channels also contribute. We include the one-loop standard model background whose interference with the graviton exchange determines the experimental reach in measuring any deviation from the standard model expectations and explore how polarization can be exploited to enhance the signal over background. We find that a 1 TeV linear collider has an experimental reach to mass scale of about 4 TeV in this channel.

I. INTRODUCTION

In the past few years the most popular speculative idea in theoretical particle physics has been the possibility that extra spacetime dimensions exist. Much of the interest in this area was stimulated by the realization that constraints on the extra dimensions were relatively mild if only gravity and not the standard model (SM) gauge interactions was able to propagate in the extra dimensions or bulk [1,2]. This led to the possibility that the effective Planck scale in the extra dimensions was much lower than the commonly used four-dimensional Planck scale. If the effective Planck scale is of order a few TeV, then speculation arose that extra dimensions might help resolve the hierarchy problem and the electroweak scale effects of the extra dimensions might appear in future collider experiments. Gauss's law links the value of the effective Planck scale in the bulk to the conventional Planck scale via

$$M_{pl}^2 \sim R^n M_S^{n+2}. \tag{1}$$

Physical effects can present themselves via graviton exchange at future colliders, and an interesting class of processes is the pair production of gauge bosons in the photon-photon collider. The process $\gamma\gamma \rightarrow \gamma\gamma$ has been studied before [3–5]. The processes $\gamma\gamma \rightarrow W^+W^-$ and $\gamma\gamma \rightarrow ZZ$ were studied in Ref. [6]. In the latter process the standard model contribution $\gamma\gamma \rightarrow ZZ$ is known [7,8] but was not included. The process $\gamma\gamma \rightarrow ZZ$ is particularly attractive for the following reasons: (1) it provides another channel with which to assess the universality of the gravitational couplings to the gauge bosons; (2) the angular dependence of $\gamma\gamma \rightarrow ZZ$ is different from $\gamma\gamma \rightarrow \gamma\gamma$ because it occurs only through the s channel while $\gamma\gamma \rightarrow \gamma\gamma$ occurs through the s, t, and u channels; (3) since only the s channel contributes to the Kaluza-Klein (KK) process of $\gamma\gamma \rightarrow ZZ$ and the KK state is spin-two, we find the only helicity amplitudes which do not vanish have opposite

initial photon helicities; (4) the Z boson's transverse and longitudinal polarizations can be exploited by measuring the angular distribution of its decay products.

An examination of all the modes $\gamma\gamma \rightarrow VV$ where $VV = ZZ$, W^+W^- and $\gamma\gamma$ will be necessary to establish the universality of the KK graviton coupling and to show its spin-two nature. Important differences between the three channels can be exploited to understand the nature of the signal. As we argue later, $\gamma\gamma \rightarrow W^+W^-$ is the channel that offers the greatest reach in probing the new physics scale (because the SM background occurs at the tree level rather than at the one-loop level and the KK graviton signal interferes with this background). If one compares $\gamma\gamma \rightarrow ZZ$ and $\gamma\gamma \rightarrow W^+W^-$, the nature of the decay products of the Z boson may allow one to better measure the production rates of the various polarization states of the Z compared to the final state W bosons in $\gamma\gamma \rightarrow W^+W^-$. So while one expects a signal to be detected first in the W^+W^- final state, the ZZ final state may offer additional experimental handles with which to study KK graviton exchange. Finally the absence of a fourth channel, $\gamma\gamma \rightarrow \gamma Z$, should also provide a strong indication that any observed signal is arising from KK graviton exchange.

Our emphasis here will be on the particular process $\gamma\gamma \rightarrow ZZ$ for which the complete calculation including the full standard model background has not been performed.[1] We also present the helicity amplitudes for $\gamma\gamma \rightarrow \gamma\gamma$ which provide a basis for comparison and also allow us to make particular points about the properties of these processes that can be exploited in a comprehensive analysis of all the final states.

*Electronic address: berger@indiana.edu
†Electronic address: bzerbe@indiana.edu

---

[1]After this work was completed, we became aware of a paper [9] which included an approximate calculation of the standard model background and calculated the helicity amplitudes. Apart from some obvious typographical errors, we agree with the angular dependences of their helicity amplitudes and obtain similar numerical results. We have in addition included the photon-photon luminosity and explored the role of polarization in isolating the signal, and have derived bounds on the scale M_S.

The standard model helicity amplitudes for $\gamma\gamma \rightarrow ZZ$ were first published in Ref. [7] and their analytic form was confirmed shortly thereafter [8]. Numerical calculations of the cross sections were also performed in Refs. [10,11]. More recently the helicity amplitudes were again derived as a background for a search for possible virtual supersymmetric particles contribution to the loop diagrams [12]. The three calculations for the analytic expressions for the matrix elements show complete agreement (apart from a typo in Ref. [7] explained in Refs. [8,12], and taking into account an unconventional definition of the Mandelstam variables t and u used in Ref. [7]). The fermion loop contribution in the standard model was first calculated [13] in the context of the gluon fusion process $gg \rightarrow ZZ$. The results for that process are easily adapted to the process considered $\gamma\gamma \rightarrow ZZ$ considered here.

At high energies where the low scale gravity signal should be most prominent, the standard model cross sections are dominated by the W loop diagrams (as one expects since the W boson is spin-one). Numerically at energies sufficiently far above threshold the cross section for the background of $\gamma\gamma \rightarrow ZZ$ is an order of magnitude larger than the background of $\gamma\gamma \rightarrow \gamma\gamma$. This can be understood simply by comparing the size of the WWZ coupling to the $WW\gamma$ where the ratio is determined solely by the Weinberg angle.

We are assuming that the effects of local higher-dimensional operators arising from the exchange of string states [14] are smaller than the KK graviton modes considered here. This is a definite assumption about the underlying theory. For details about the possible stringy effects that might arise one can consult Ref. [14] which includes a discussion regarding the particular case of $\gamma\gamma \rightarrow \gamma\gamma$.

Photon beams can be realized at a future e^+e^- collider by Compton backscattering laser beams off the electron or positron beam [15–17]. By exploiting circular polarization of the lasers and polarizing the electron beams, the contribution to cross sections from various initial state photon helicities can be adjusted.

We have obtained the contributions for the graviton exchange signal for both $\gamma\gamma \rightarrow \gamma\gamma$ and $\gamma\gamma \rightarrow ZZ$ at the helicity amplitude level through the use of FORM [18]. If the photon-photon option at a next generation linear collider becomes a real possibility in the future, this will facilitate detailed investigations of these processes putting in the full interference with the standard model contributions and retaining all information on the polarization of the incident photon beams. Furthermore, for the ZZ final state, more sophisticated cuts on the Z boson decay products via the density matrix formalism can be exploited to improve sensitivity to any signal. Finally, having the helicity amplitudes at our disposal allows us to understand angular distributions that reflect the fact that graviton exchange is spin-two in nature.

Other processes have been considered as probes of low scale gravity. For cases where gravitons appear as virtual particles, calculations have been performed for the production of fermions [19,20], gauge bosons [21,22], Higgs bosons [23], and final states beyond pair production [24]. The general helicity formalism for spin-two particles has been developed in Ref. [25].

Constraints have also been placed on these theories of extra dimensions by testing the gravitational inverse-square law. The case of $n = 1$ is already ruled out by solar system observations, and tests at the submillimeter level [26] can provide bounds at the TeV level. Furthermore strong constraints ($\gtrsim 100$ TeV) can be obtained for $n = 2$ from effects on the KK gravitons on the cooling in SN1987a [27] and considering the graviton decay contribution to the cosmic diffuse gamma radiation [28]. More recent analysis and review of the supernova and neutron star limits for various values of n can be found in Ref. [29].

II. HELICITY AMPLITUDES FOR $\gamma\gamma \rightarrow \gamma\gamma$

Feynman rules have been developed for the KK compactification of n extra dimensions on a torus T^n with all of the n compactification radii equal [30]. Using the couplings of the $d = 4$ gauge fields to gravity, one can analyze the possible effects of low scale gravity on gauge boson scattering. Since this phenomenology involves the exchange of massive spin-two KK states, there is a possibility of unique angular dependences in cross sections involving the exchange of these quanta.

We define momentum and polarization vectors for the initial and final particles as[2]

$$p_1 = \frac{\sqrt{s}}{2}(1;0,0,1) \quad p_2 = \frac{\sqrt{s}}{2}(1;0,0,-1)$$

$$k_1 = \frac{\sqrt{s}}{2}(1;\beta\sin\theta,0,\beta\cos\theta)$$

$$k_2 = \frac{\sqrt{s}}{2}(1;-\beta\sin\theta,0,-\beta\cos\theta)$$

$$e_1^+ = e_2^- = \frac{1}{\sqrt{2}}(0;-1,-i,0) \quad e_1^- = e_2^+ = \frac{1}{\sqrt{2}}(0;1,-i,0)$$

$$e_3^{+*} = e_4^{-*} = \frac{1}{\sqrt{2}}(0;-\cos\theta,i,\sin\theta)$$

$$e_3^{-*} = e_4^{+*} = \frac{1}{\sqrt{2}}(0;\cos\theta,i,-\sin\theta)$$

$$e_3^0 = \frac{\sqrt{s}}{2m_z}(\beta;\sin\theta,0,\cos\theta)$$

$$e_4^0 = \frac{\sqrt{s}}{2m_z}(\beta;-\sin\theta,0,-\cos\theta),$$

where $\beta = 1$ for the $\gamma\gamma \rightarrow \gamma\gamma$ case and $\beta = \sqrt{1-(4M_Z^2)/s}$

---

[2]This choice of polarization vectors is the same as the one in Ref. [7]. Our definitions of the Mandelstam variables require switching t and u when comparing with that paper.

for the $\gamma\gamma \rightarrow ZZ$ case, $s = (p_1 + p_2)^2$, $t = (p_1 - k_1)^2$, and $u = (p_1 - k_2)^2$.

The process $\gamma\gamma \rightarrow \gamma\gamma$ can be expressed in terms of three independent helicity amplitudes. The other helicity amplitudes are related to these three by virtue of crossing relations and parity considerations. For the graviton exchange signal, we find that only two of these three are nonvanishing,

$$i\mathcal{M}_{++++}^{\gamma\gamma} = -\frac{\kappa^2}{2}(D_E(t) + D_E(u))s^2, = -\frac{\kappa^2}{2}\left(D_E\left(-\frac{s}{2}(1-\cos\theta)\right) + D_E\left(-\frac{s}{2}(1+\cos\theta)\right)\right)s^2,$$

$$i\mathcal{M}_{++--}^{\gamma\gamma} = -\frac{\kappa^2}{4}(D_E(t) - D_E(u))(u^2 - t^2) = -\frac{\kappa^2}{4}\left(D_E\left(-\frac{s}{2}(1-\cos\theta)\right) - D_E\left(-\frac{s}{2}(1+\cos\theta)\right)\right)s^2\cos\theta, \quad (2)$$

$$i\mathcal{M}_{+++-}^{\gamma\gamma} = 0,$$

where $D(x)$ for $x = s$ and $D_E(x)$ for $x = t, u$ are the summed propagator functions[3] derived in Ref. [30] and $\kappa = \sqrt{16\pi G_N}$. We have therefore used the full expression for $D(s)$ for our analysis of the $\gamma\gamma \rightarrow ZZ$ process, which is

$$D(s) = \frac{s^{(n/2)-1}R^n}{(4\pi)^{n/2}\Gamma(\frac{n}{2})}\left(\pi + 2iI\left(\frac{M_S}{\sqrt{s}}\right)\right), \quad (5)$$

where

$$I(x) = \begin{cases} -\sum_{k=1}^{(n/2)-1}\frac{1}{2k}x^{2k} - \frac{1}{2}\log(x^2 - 1) & n = \text{even} \\ -\sum_{k=1}^{[(n-1)/2]-1}\frac{1}{2k-1}x^{2k-1} + \frac{1}{2}\log\left(\frac{x+1}{x-1}\right) & n = \text{odd}, \end{cases} \quad (6)$$

and

$$D_E(t) = \frac{|t|^{(n/2)-1}R^n}{(4\pi)^{n/2}\Gamma(\frac{n}{2})}\left(-2iI_E\left(\frac{M_S}{\sqrt{|t|}}\right)\right), \quad (7)$$

where

$I_E(x)$

$$= \begin{cases} (-1)^{(n/2)+1}\sum_{k=1}^{(n/2)-1}\frac{(-1)^k}{2k}x^{2k} + \frac{1}{2}\log(x^2 + 1) & n = \text{even} \\ (-1)^{(n-1)/2}\sum_{k=1}^{(n-1)/2}\frac{(-1)^k}{2k-1}x^{2k-1} + \tan^{-1}(x) & n = \text{odd}. \end{cases} \quad (8)$$

The scale M_S is defined as

$$R^n = \frac{(4\pi)^{n/2}\Gamma(n/2)}{2M_S^{n+2}G_N}, \quad (9)$$

___

[3]We find the sometimes used approximations

$$\kappa^2 D(s) \approx -\frac{16\pi i}{M_S^4}\mathcal{F}, \quad (3)$$

where

$$\mathcal{F} = \begin{cases} \log\left(\frac{M_S^2}{s}\right) & \text{for } n = 2 \\ \frac{2}{n-2} & \text{for } n > 2 \end{cases} \quad (4)$$

can cause deviations from the exact expressions of tens of percent in the cross section.

where $G_N = 1/(8\pi\bar{M}_{pl}^2)$ is the 4-dimensional Newton's constant, where $\bar{M}_{pl} = 2.4 \times 10^{18}$ GeV is the reduced Planck mass. This definition for the mass scale M_S is the one of Han, Lykken, and Zhang [30] and makes precise the relationship in Eq. (1). Other possible conventions for the mass scale were considered in Refs. [19,31] and should not be confused with the one chosen here.

The amplitudes $\mathcal{M}_{++++}^{\gamma\gamma}$ and $\mathcal{M}_{+-+-}^{\gamma\gamma}$ and also $\mathcal{M}_{++++}^{\gamma\gamma}$ and $\mathcal{M}_{+--+}^{\gamma\gamma}$ are related by crossing

$$\mathcal{M}_{+--+}^{\gamma\gamma}(s, t, u) = \mathcal{M}_{++++}^{\gamma\gamma}(u, t, s),$$

$$\mathcal{M}_{+-+-}^{\gamma\gamma}(s, t, u) = \mathcal{M}_{++++}^{\gamma\gamma}(t, s, u). \quad (10)$$

It is also noteworthy that the matrix element $\mathcal{M}_{++--}$ vanishes in the approximation $D(s) \approx D_E(|t|) \approx D_E(|u|)$.

Representing the initial and final helicity states of the photons as $\lambda_1\lambda_2$ and $\lambda_3\lambda_4$, respectively, the other four nonzero helicity amplitudes can be expressed in terms of one of the previous amplitudes through

$$\mathcal{M}_{\lambda_1\lambda_2\lambda_3\lambda_4}^{\gamma\gamma}(s, t, u) = \mathcal{M}_{-\lambda_1-\lambda_2-\lambda_3-\lambda_4}^{\gamma\gamma}(s, t, u), \quad (11)$$

$$\mathcal{M}_{\lambda_1\lambda_2\lambda_3\lambda_4}^{\gamma\gamma}(s, t, u) = \mathcal{M}_{\lambda_2\lambda_1\lambda_4\lambda_3}^{\gamma\gamma}(s, t, u), \quad (12)$$

which are results of Bose symmetry and parity. The angular dependence of these matrix elements are in agreement with the results of Ref. [21].

By squaring and summing these matrix elements and making the approximation as in Eq. (3), the polarization averaged result for the signal only (without the standard model background) can be derived, namely

$$\frac{1}{4}\sum|\mathcal{M}^{\gamma\gamma}|^2 = \frac{\kappa^4}{2}|D(s)|^2(s^4 + t^4 + u^4). \quad (13)$$

The factor $\frac{1}{4}$ is the initial state photon polarization average. This is in agreement with the corresponding result in Ref. [3] if an erroneous factor of one-half in the KK propagator of an earlier version of Ref. [30] is omitted. Furthermore, our result agrees with the expression of Ref. [3] when written in terms of M_S.

The signal represented by these amplitudes for $\gamma\gamma \rightarrow \gamma\gamma$ at photon-photon colliders has been studied before [3–5]. Explicit analytic expressions for the helicity amplitudes

allow one to understand more fully the optimal strategy for exploiting polarization to optimize the sensitivity. In our discussion of the process $\gamma\gamma \rightarrow ZZ$ beginning in the next section, we will be able to compare to the simpler case of $\gamma\gamma \rightarrow \gamma\gamma$ and highlight some important contrasts. A detailed analysis of $\gamma\gamma \rightarrow \gamma\gamma$ as a mode to study exchange of KK states at photon-photon colliders will appear elsewhere [32].

III. HELICITY AMPLITUDES FOR $\gamma\gamma \rightarrow ZZ$

The graviton exchange Feynman rules for the $\gamma\gamma \rightarrow ZZ$ process is similar to the $\gamma\gamma \rightarrow \gamma\gamma$ case except for the restriction of the process to the s channel. This restriction is due to the fact that there is no interaction vertex between γ, Z, and the KK state. We define

$$s_4 = s - 4M_Z^2, \qquad Y = tu - M_Z^4 = s \cdot p_{TZ}^2, \qquad (14)$$

where p_{TZ} is the transverse momentum of either Z. For the TT polarization modes (the notation T denotes collectively the two transverse polarizations ($+$ and $-$) of the Z boson and L will denote the longitudinal polarization (0)). For the final state Z bosons, we obtained[4]

$$i\mathcal{M}_{+-++} = i\mathcal{M}_{+---} = -D(s)2\kappa^2 \frac{Y}{s_4} M_Z^2$$

$$= -D(s)\frac{\kappa^2 M_Z^2 s}{2}\sin^2\theta, \qquad (15)$$

$$i\mathcal{M}_{+--+} = D(s)\frac{\kappa^2}{4\beta^3}(2\beta M_Z^4 - 2(t-u)M_Z^2 - t^2(1+\beta)$$

$$+ u^2(1-\beta))$$

$$= -D(s)\frac{\kappa^2 s^2}{8}(1-\cos\theta)^2, \qquad (16)$$

$$i\mathcal{M}_{+-+-} = D(s)\frac{\kappa^2}{4\beta^3}(2\beta M_Z^4 - 2(u-t)M_Z^2 - u^2(1+\beta)$$

$$+ t^2(1-\beta))$$

$$= -D(s)\frac{\kappa^2 s^2}{8}(1+\cos\theta)^2. \qquad (17)$$

The amplitudes $\mathcal{M}_{+-+-}$ and $\mathcal{M}_{+--+}$ are related either by $t \leftrightarrow u$ or by $\beta \rightarrow -\beta$. For the LL final state polarization mode, we obtained

$$i\mathcal{M}_{+-00} = D(s)\frac{\kappa^2 Y}{2s_4}(s + 4M_Z^2)$$

$$= D(s)\frac{\kappa^2 s}{8}(s + 4M_Z^2)\sin^2\theta. \qquad (18)$$

Finally for the TL final state polarization modes, we ob-

---

[4]We have chosen to denote the helicity amplitudes for $\gamma\gamma \rightarrow \gamma\gamma$ by $\mathcal{M}^{\gamma\gamma}$ and those for our main focus $\gamma\gamma \rightarrow ZZ$ without any superscript.

tained

$$i\mathcal{M}_{+-+0} = -i\mathcal{M}_{+-0-} = -D(s)\frac{\kappa^2 \Delta Y}{\beta^2}\left(\beta + \frac{t-u}{s}\right)$$

$$= -D(s)\frac{\kappa^2 M_Z s}{2}\sqrt{\frac{s}{2}}\sin\theta(1+\cos\theta), \qquad (19)$$

$$i\mathcal{M}_{+--0} = -i\mathcal{M}_{+-0+} = -D(s)\frac{\kappa^2 \Delta Y}{\beta^2}\left(\beta + \frac{u-t}{s}\right)$$

$$= -D(s)\frac{\kappa^2 M_Z s}{2}\sqrt{\frac{s}{2}}\sin\theta(1-\cos\theta), \qquad (20)$$

with $\Delta = \sqrt{(sM_Z^2)/(2Y)}$. Other helicity modes can be obtained from these by using equations analogous to Eqs. (11) and (12). The first of these equations must be modified to account for the possibility of the TL final state

$$\mathcal{M}_{\lambda_1\lambda_2\lambda_3\lambda_4}(s, t, u, \beta) = \mathcal{M}_{-\lambda_1-\lambda_2-\lambda_3-\lambda_4}(s, t, u, \beta)$$

$$\times (-1)^{\lambda_3-\lambda_4}, \qquad (21)$$

$$\mathcal{M}_{\lambda_1\lambda_2\lambda_3\lambda_4}(s, t, u, \beta) = \mathcal{M}_{\lambda_2\lambda_1\lambda_4\lambda_3}(s, t, u, \beta). \qquad (22)$$

This amounts to an extra minus sign only. One can also obtain a relation between TL amplitudes that amounts to taking $\beta \rightarrow -\beta$, but we have chosen to display these helicity amplitudes separately to emphasize their relationship under the interchange $t \leftrightarrow u$.

Helicity modes $\mathcal{M}_{-+\lambda_3\lambda_4}$ can be obtained from the corresponding amplitudes $\mathcal{M}_{+-\lambda_3\lambda_4}$. All other independent helicity amplitudes vanish; in particular, the signal vanishes if the initial photons have the same helicity. We again find agreement with the angular dependence of these helicity amplitudes with those in Ref. [21].

At high energies ($\sqrt{s} \gg M_Z$) the standard model background is dominated by Z bosons in the transverse polarization states. There are contributions from all initial helicity possibilities of the incident photons. The Higgs boson contributes only to channels in which the two initial photons have the same helicity ($\lambda_1 = \lambda_2$) and the final state Z bosons must have the same helicities ($\lambda_3 = \lambda_4$). This property reflects the fact that the Higgs boson is spin-zero, and while the Higgs boson does not appreciably affect the results for the low scale gravity signal, we mention it here to contrast it with the spin-two nature of the s-channel graviton exchange graphs.

The s-channel graviton exchange graphs require differing helicities ($\lambda_1 = -\lambda_2$) for the initial photons. The dominant matrix elements for high energies ($\sqrt{s} \gg M_Z$) are $\mathcal{M}_{+-+-}$, $\mathcal{M}_{+--+}$ and $\mathcal{M}_{+-00}$ which have the following angular dependences respectively: $t^2 = \frac{s^2}{4} \times (1-\cos\theta)^2$, $u^2 = \frac{s^2}{4}(1+\cos\theta)^2$, and $tu = \frac{s^2}{4}\sin^2\theta$. The absence of a signal in channels where the initial photons have the same helicity differs from the $\gamma\gamma \rightarrow \gamma\gamma$ case, because in addition to the s-channel diagram, the $\gamma\gamma \rightarrow \gamma\gamma$ process has additional contributions from the t and u channels. This impacts the analysis in two ways: (1) For

$\gamma\gamma \to ZZ$ one can try to isolate the signal by arranging the initial state helicities of the incoming photons to be opposite. This can be done by appropriately choosing the initial electron and positron polarizations as well as the polarization of the backscattered laser beams. (2) The signal for $\gamma\gamma \to ZZ$ is somewhat smaller than the signal for $\gamma\gamma \to \gamma\gamma$ expressed in Eq. (13). This makes finding a signal harder, and weakens the overall bound one could otherwise place on the scale M_S.

Since the interference between the signal and the background can be crucial to the detectability of any signal, it is important to examine not only their overall sizes but also their relative phases. At large energies, $s \gg M_Z^2$, the standard model background is dominated by the W boson loops, and these dominant contributions become predominantly imaginary.[5] The signal involves the propagator function [30]

$$D(s) = \sum_{\vec{n}} \frac{i}{s - m_{\vec{n}} + i\epsilon}. \tag{23}$$

Using

$$\frac{1}{s - m^2 + i\epsilon} = P\left(\frac{1}{s - m^2}\right) - i\pi\delta(s - m^2) \tag{24}$$

yields the expression in Eq. (5), and one recognizes that the imaginary part of $D(s)$ contributes to the real part of the helicity amplitudes, and the real part of $D(s)$ contributes to the imaginary part of the helicity amplitudes. Physically speaking, the imaginary part of $D(s)$ involving $I(M_S/\sqrt{s})$ arises from the (coherent) summation of the large number of nonresonant states and typically dominates for $s \ll M_S^2$. So in the physical region we are contemplating looking for a graviton exchange signal, $M_Z^2 \ll s \ll M_S^2$, the background is mostly imaginary and the signal is mostly real. One point that should not be overlooked is that the approximation for $D(s)$ sometimes employed not only makes an approximation for the imaginary part, but also completely drops the real part which can still have a significant interference with the W loop standard model background. However it should be kept in mind that the W loop background approaches its asymptotic behavior rather slowly, so the interference can still remain nonnegligible in practice especially for the realistic case of $\sqrt{s_{ee}} = 1$ TeV.

We find the TL polarization modes for the final state Z bosons to be nonzero, but suppressed at high energies relative to the dominant helicity amplitudes identified above by a factor $M_Z/\sqrt{s}$. These polarization modes are of course absent in the case of final state photons in $\gamma\gamma \to \gamma\gamma$. Finally the TT polarization modes $\mathcal{M}_{+-++}$ and $\mathcal{M}_{+---}$ are suppressed by a factor M_Z^2/s because it requires that the Z bosons have the same helicity. This

---

[5]For explicit expressions, see, for example, Eq. (3.26) of Ref. [7] or Eq. (10) of Ref. [33].

amplitude would vanish in the limit where M_Z is taken to zero.

IV. SIGNAL AND BACKGROUND

Sources of high energy photons can be obtained by backscattering laser photons of energy a few electron volts off high energy beams of electrons or positrons. Such colliders have come to be called photon-photon colliders or $\gamma\gamma$ colliders. This technique allows a much harder spectrum of photons than is available in the usual Weizsäcker-Williams spectrum. In fact, photon-photon collisions with energies almost the same order as the parent e^+e^- collider can be obtained. Furthermore, polarization of the electron and positron beams together with polarization of the lasers can yield polarized photon beams. Therefore, by adjusting these polarizations, one can enhance or suppress matrix elements with differing initial state photon helicities. In the case of the ZZ (and W^+W^-) final states, one can also in principle use the differing decay distributions to study the polarization states of the final state gauge bosons. This technique has not been employed in this analysis; we have imposed instead a simple angular cut on the produced Z bosons.

The subprocess cross sections are given by $d\hat{\sigma}_{++}$ and $d\hat{\sigma}_{+-}$ where the final state polarizations have been summed over. After folding in the photon luminosity functions $f(x_i)$ and $\xi(x_i)$ for $i = 1, 2$, one obtains the differential cross section as

$$
\begin{aligned}
d\sigma_{\lambda_3\lambda_4} = &\int_{M_Z^2/s_{ee}}^{y_m^2} d\tau \int_{\tau/y_m}^{y_m} \frac{dy}{y} f(y) f(\tau/y) \\
&\times \left[\frac{1}{2}\{1 + \xi(y)\xi(\tau/y)\}d\hat{\sigma}_{++\lambda_3\lambda_4}(s_{\gamma\gamma}) \right. \\
&\left. + \frac{1}{2}\{1 - \xi(y)\xi(\tau/y)\}d\hat{\sigma}_{+-\lambda_3\lambda_4}(s_{\gamma\gamma}) \right],
\end{aligned} \tag{25}
$$

where $y = E_\gamma/E_e$ and $\tau = s_{\gamma\gamma}/s_{ee}$ are the ratios of photon energies to the parent electron/positron energies. The energy spectrum and helicity of backscattered photons, $f(y)$ and $\xi(y)$, are given in Refs. [15–17]. We have taken the usual choice where the laser energy ω_0 is chosen so that $x = 4E_e\omega_0/m_e^2 = 2(1 + \sqrt{2}) \approx 4.8$ and $y_m = x/(x + 1) \approx 0.83$.

The standard model background for $\gamma\gamma \to ZZ$ (and $\gamma\gamma \to \gamma\gamma$) is dominated by only a few helicity amplitudes at high energies. For equal initial photon helicities the contribution to the cross section from the amplitude $\mathcal{M}_{++++}$ is more than an order of magnitude larger than any other contribution even after a reasonable angular cut on the final state Z bosons. Similarly in the unequal initial photon helicity case the contribution to the cross section is dominated by the two amplitudes $\mathcal{M}_{+-+-}$ and $\mathcal{M}_{+-+-}$. The cross section for longitudinally polarized Z bosons arising from $\mathcal{M}_{+-00}$ is at least an order of magnitude smaller for $\sqrt{s} > 500\gamma\gamma$ GeV.

These amplitudes are dominated at high energies by the W loop contributions (as opposed to the fermion loop diagrams), so the relative size of the cross sections for $\gamma\gamma \to \gamma\gamma$ and $\gamma\gamma \to ZZ$ is easily estimated in this limit. One simply substitutes for the relative sizes of the $\gamma\gamma W$ and ZZW couplings: $\sigma(\gamma\gamma \to \gamma\gamma) = \tan^4\theta_W \sigma(\gamma\gamma \to ZZ)$, and the ZZ final state is enhanced by a factor of about 12.

The fact that the signal for graviton exchange contributes only to helicity amplitudes with unequal initial photon helicities can be exploited experimentally. By selecting the electron, positron, and laser polarizations to give the desired initial photon helicities, one can suppress the large background arising from $\mathcal{M}_{++++}$ while enhancing the signal. In contrast the process $\gamma\gamma \to \gamma\gamma$ has signal contributions in both same and opposite initial photon helicity channels.

We have assumed a Higgs boson mass of $M_H = 150$ GeV to make the plots. A higher Higgs mass would appear as a resonance in some of the cross sections (σ_{++00}, σ_{++++}, and σ_{++--}) but, since the resonance is a small fraction of the background for any $M_H > 400$ GeV, the exact value of the Higgs mass is completely irrelevant for determining the size of the graviton signal plus background considered here. Similarly in the region where $\sqrt{s_{\gamma\gamma}}$ is several hundred TeV, the standard model W loop background completely dominates over the fermion loops. Nevertheless we mention that we have used a top quark mass of $m_t = 175$ GeV, and occasionally one can notice a change in behavior in the standard model background at the threshold $\sqrt{s_{\gamma\gamma}} = 2m_t$.

The cross section for various helicity combinations of the initial state photons and final state Z bosons are shown in Figs. 1–5 for the standard model background and for the graviton exchange signal plus background for $n = 4$ and for $M_S = 3, 4, 5, 6$ TeV. We have employed an angular cut on the c.m. scattering angle of $|\cos\theta| < \cos(\pi/6)$. The signal is dominated by the cross sections σ_{+-+-}, σ_{+--+}, and σ_{+-00} shown in Figs. 1 and 2. For large $\sqrt{s_{\gamma\gamma}}$ ($\sqrt{s_{\gamma\gamma}} \gg M_z$), the cross sections grow like $s_{\gamma\gamma}^3/M_S^8$. Moreover, for such large energy the TL final state signals shown in Fig. 3 grow like $s_{\gamma\gamma}^2 M_Z^2/M_S^8$ while the remaining TT amplitudes shown in Fig. 4 grows like $s_{\gamma\gamma} M_Z^4/M_S^8$ for large $s_{\gamma\gamma}$. When the signal and background are of comparable size ($\sqrt{s_{\gamma\gamma}} \lesssim 1$ TeV), the contribution from the transverse states shown in Fig. 1 will dominate the signal since the interference with the underlying standard model background determines its overall size. Therefore it is important to include the interference between the signal and background when estimating the reach of possible future experimental searches.

The background consists of the standard model contributions from the opposite photon helicity ($\lambda_1 = -\lambda_2$) modes shown in Figs. 1–4 as well as from the same photon helicity ($\lambda_1 = \lambda_2$) modes shown in Fig. 5 which, as pre-
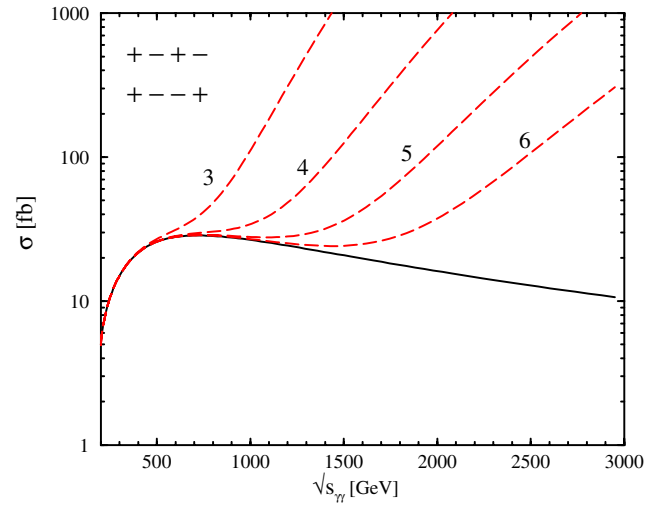

FIG. 1 (color online). The cross section is shown for $\sigma_{+-+-} = \sigma_{+--+}$ for the standard model background (solid) and for signal plus background (dashed) for $n = 4$ and $M_S = 3$, 4, 5, and 6 TeV from top to bottom. The signal cross sections grow like s^3/M_S^8 in the region $M_Z^2 \ll s \ll M_S^2$. A cut has been placed on the c.m. scattering angle $|\cos\theta| < \cos(\pi/6)$.

viously mentioned, do not receive contributions from the spin-two graviton exchange. The background is dominated by the cross section σ_{++++} which can exceed 100 femtobarns. Unlike the process $\gamma\gamma \to \gamma\gamma$ there is no signal contribution in this mode for $\gamma\gamma \to ZZ$ because the latter only proceeds via the s channel. Furthermore the overall size of $\gamma\gamma \to ZZ$ is larger than $\gamma\gamma \to \gamma\gamma$ due to enhanced WWZ coupling. For most practical purposes the overall
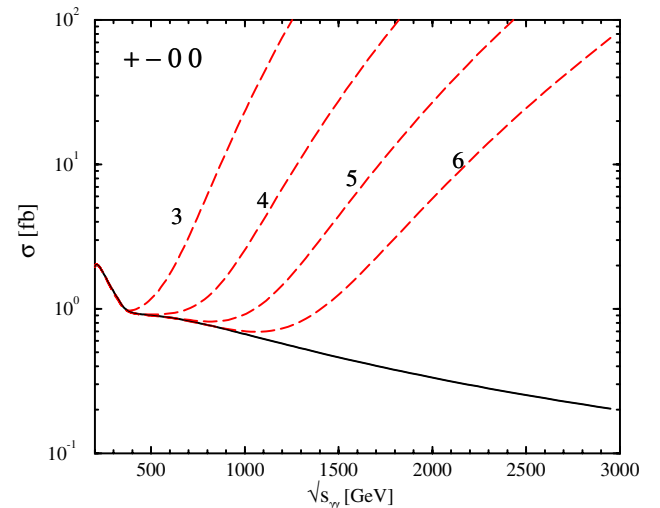

FIG. 2 (color online). The cross section is shown for σ_{+-00} for the standard model background (solid) and for signal plus background (dashed) for $n = 4$ and $M_S = 3$, 4, 5, and 6 TeV from top to bottom. The signal cross section grows like s^3/M_S^8 in the region $M_Z^2 \ll s \ll M_S^2$. A cut has been placed on the c.m. scattering angle $|\cos\theta| < \cos(\pi/6)$.
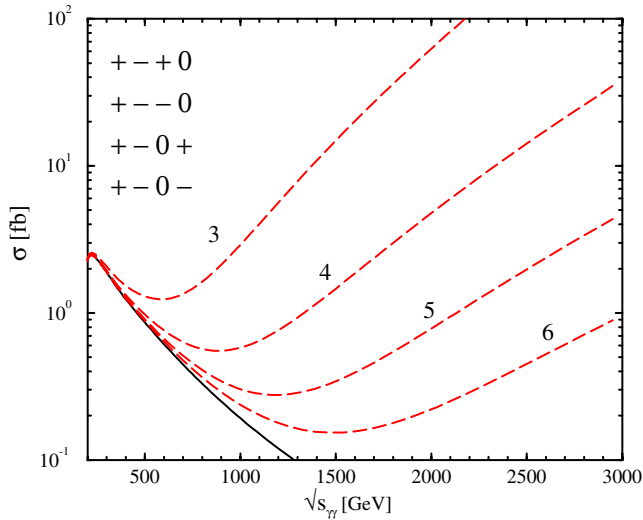
FIG. 3 (color online). The cross section is shown for $\sigma_{+-+0} = \sigma_{+-0-}$ ($\approx \sigma_{+-0+} = \sigma_{+--0}$) for the standard model background (solid) and for signal plus background (dashed) for $n = 4$ and $M_S = 3, 4, 5,$ and 6 TeV from top to bottom. The signal cross sections grow like $s^2 M_Z^2/M_S^8$ in the region $M_Z^2 \ll s \ll M_S^2$. A cut has been placed on the c.m. scattering angle $|\cos\theta| < \cos(\pi/6)$.

FIG. 5. The cross sections for the case of equal photon helicities are shown. Since the gravitation signal does not contribute to these modes, what is shown arises from the standard model alone and contributes only as background. Notice the wide range of scales and the dominance of σ_{++++} for the larger $\sqrt{s_{\gamma\gamma}}$ of interest. At the lower left the unlabeled curves correspond to σ_{++--} (the larger one) and σ_{++-0} (the smaller one). A cut has been placed on the c.m. scattering angle $|\cos\theta| < \cos(\pi/6)$.

level of the signal and background can be estimated by concentrating attention on the contributions in Figs. 1 and 5 which dominate in most cases. We do not present a figure summing these contributions since the optimal strategy for uncovering the signal will be to use polarization to isolate
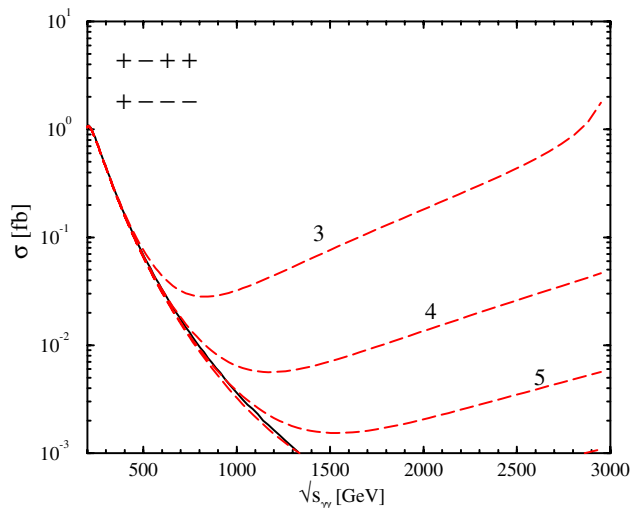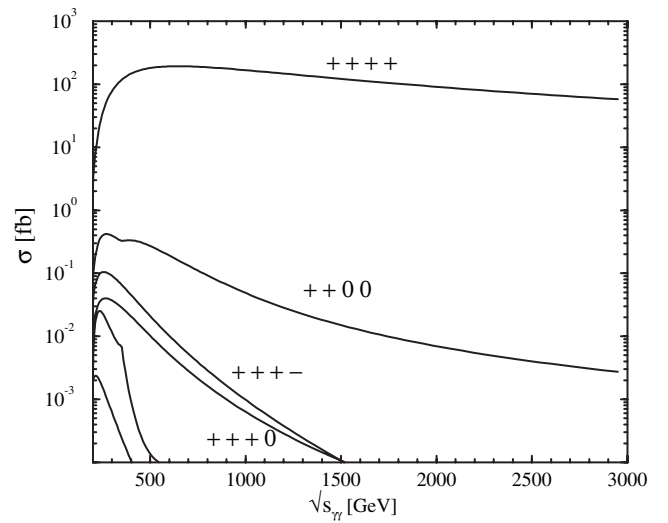
the helicity amplitudes containing the signal as outlined in detail below.

In Fig. 6 the effect of varying the number of extra dimensions n is shown keeping the scale M_S fixed at 4 TeV. We show only the most important modes, namely $\sigma_{+-+-} = \sigma_{+--+}$ in Fig. 6(a) and σ_{+-00} in Fig. 6(b). The conclusion is that stronger bounds can be placed when n is smaller.

The strategy of choosing polarizations to optimize the signal over background is particularly simple for the process $\gamma\gamma \to ZZ$. The graviton exchange signal requires opposite helicities for the initial state photons, so one should choose polarizations for the electron and positron beams as well as the laser beams to isolate this combination and to eliminate as much as possible the large background from σ_{++++}. We denote the polarizations of the electron (e_1), positron (e_2), and laser beams (γ_1 and γ_2) by ($P_{e_1}, P_{\gamma_1}, P_{e_2}, P_{\gamma_2}$). At a photon-photon collider the luminosity is rather flat for the unpolarized case, and one achieves a peak in the luminosity just below the maximum energy by choosing opposite polarizations for the electron and laser photon, e.g. in the ideal case $P_{e_1}P_{\gamma_1} = -1$ and $P_{e_2}P_{\gamma_2} = -1$ (see, for example, Fig. 11 of Ref. [17]). Since one wants to look for a rapidly growing signal on top of a standard model background, clearly the optimal situation occurs when the luminosities are concentrated at the highest energies possible. In addition, to isolate the opposite photon helicity amplitudes, one wants to choose the polarizations such that $P_{e_1} = -P_{e_2}$ and $P_{\gamma_1} = -P_{\gamma_2}$.

FIG. 4 (color online). The cross section is shown for $\sigma_{+-++} = \sigma_{+---}$ for the standard model background (solid) and for signal plus background (dashed) for $n = 4$ and $M_S = 3,$ 4, and 5 TeV from top to bottom. The signal cross section grows like $s M_Z^4/M_S^8$ in the region $M_Z^2 \ll s \ll M_S^2$. A cut has been placed on the c.m. scattering angle $|\cos\theta| < \cos(\pi/6)$.
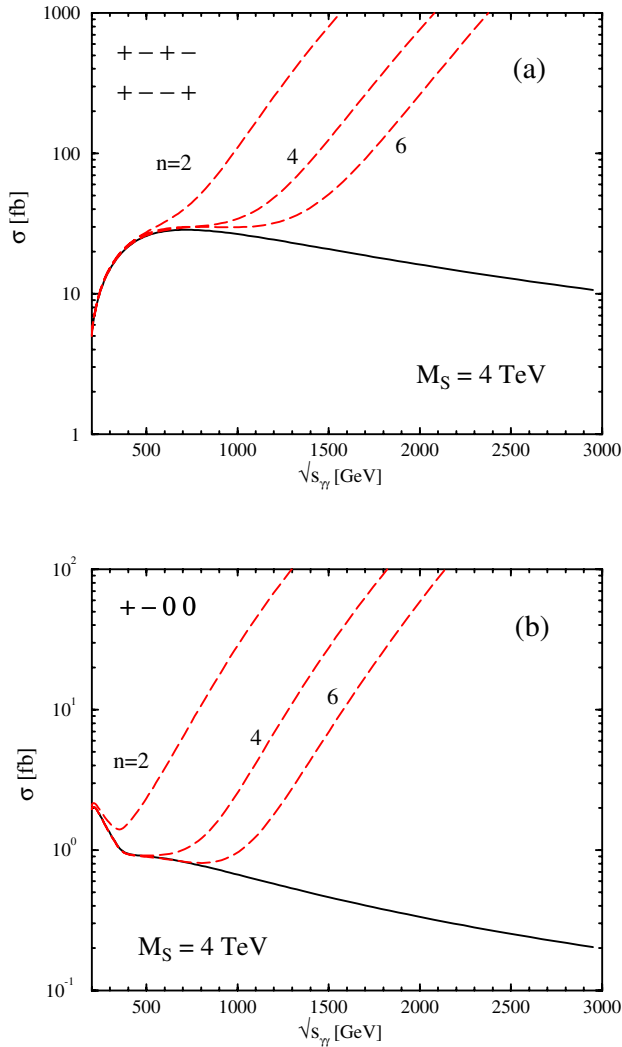
FIG. 6 (color online). The cross sections are shown for (a) $\sigma_{+-+-} = \sigma_{+--+}$ and (b) σ_{+-00} for the standard model background (solid) and for signal plus background (dashed) for $M_S = 4$ TeV and the number of extra dimensions $n = 2$, 4, and 6.
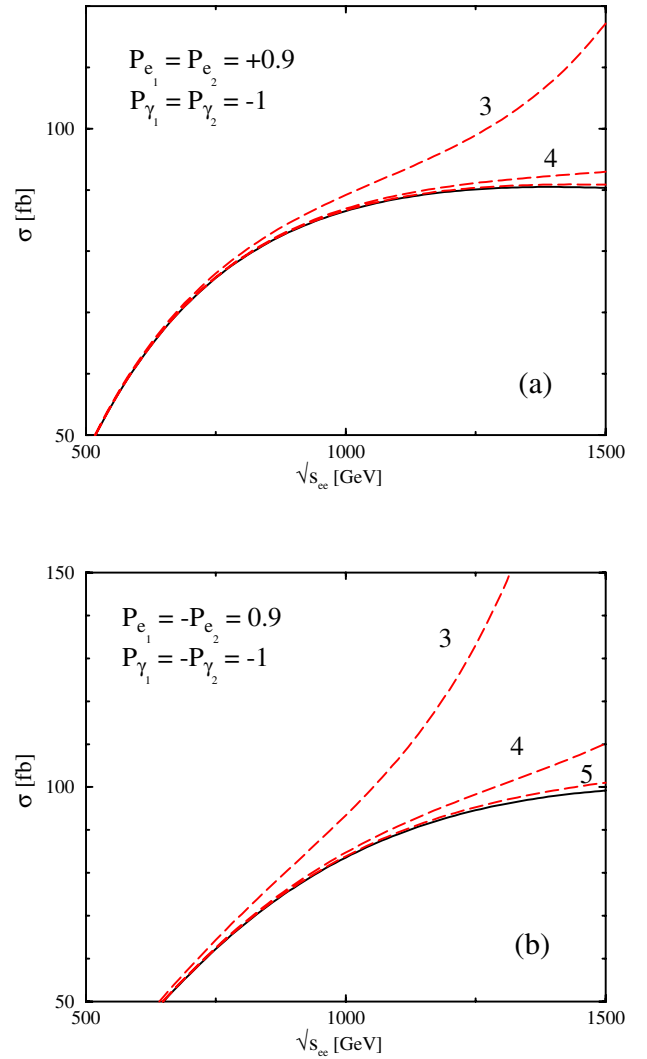

FIG. 7 (color online). The cross sections are shown for a photon-photon collider whose parent $e^+ e^-$ collider has energy $\sqrt{s_{ee}}$ for the choice of polarizations (a) $(P_{e_1}, P_{\gamma_1}, P_{e_2}, P_{\gamma_2}) = (+, -, +, -)$ and (b) $(P_{e_1}, P_{\gamma_1}, P_{e_2}, P_{\gamma_2}) = (+, -, -, +)$, and for $M_S = 3, 4, 5$ TeV. The number of extra dimensions is $n = 4$. The polarization in (a) favors backscattered photons with the same helicity while (b) favors backscattered photons with opposite helicities.

Therefore we have assumed in the following analysis that the electron/positron beams can be polarized to 90%, and assume the photon-photon collider has the following polarization combinations:

$$P_{e_1} = -P_{e_2} = 0.9, \qquad P_{\gamma_1} = -P_{\gamma_2} = -1. \qquad (26)$$

This polarization setting will be denoted by the shorthand $(P_{e_1}, P_{\gamma_1}, P_{e_2}, P_{\gamma_2}) = (+, -, -, +)$. It was noticed in Ref. [6] that this kind of polarization enhanced the signal for the process $\gamma\gamma \to W^+W^-$. This can be understood on the basis of our helicity amplitudes for $\gamma\gamma \to ZZ$ which can be converted into helicity amplitudes for $\gamma\gamma \to W^+W^-$ with minor modifications since both processes occur via only the s channel. The standard model background for $\gamma\gamma \to W^+W^-$ occurs at tree level rather than at one loop as it does for $\gamma\gamma \to ZZ$, so the reach is expected

to be higher in W production since the interference of the signal with the background is crucial.

The polarization setting that has the photon-photon luminosity peaking at the highest energy but gives predominantly backscattered photons with the same helicity is $(P_{e_1}, P_{\gamma_1}, P_{e_2}, P_{\gamma_2}) = (+, -, +, -)$. This polarization setting would be optimal for a case where a signal contributed to the helicity amplitudes $\mathcal{M}_{++\lambda_3\lambda_4}$. Thus this setting would be preferable for the $\gamma\gamma \to \gamma\gamma$ process, which is consistent with the results of the calculations in Ref. [4].

In Fig. 7 a comparison is made between the two polarization settings. One observes a noticeable improvement in
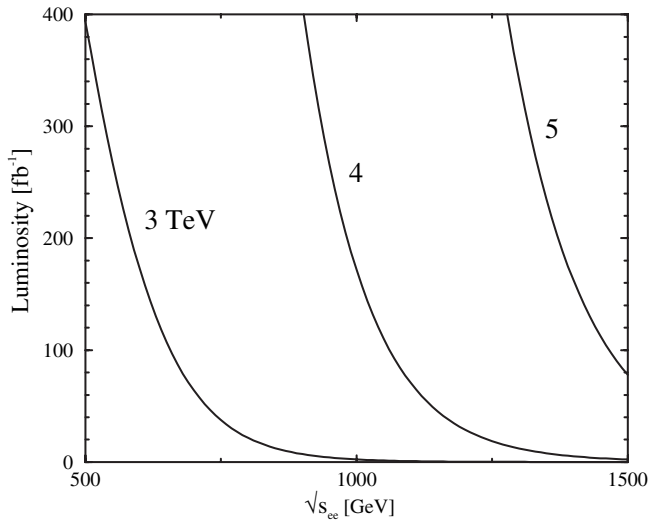
FIG. 8.   The luminosity required to detect a signal at the 95% confidence level for $M_S = 3, 4, 5$ TeV as a function of $\sqrt{s_{ee}}$ with the polarization choice $(P_{e_1}, P_{\gamma_1}, P_{e_2}, P_{\gamma_2}) = (+, -, -, +)$ as in Fig. 7(b). The number of extra dimensions in $n = 4$.

the second polarization choice. For this choice we have determined the integrated luminosity required to observe at the 95% confidence level a signal over the standard model background for three choices of M_S. This is shown in Fig. 8 for the case of $n = 4$. In particular, with an integrated luminosity of 100 fb^{-1}, a linear collider with c.m. energy of 1 TeV has a reach almost up to $M_S = 4$ TeV. This determination of the experimental reach for the case of $\gamma\gamma \rightarrow ZZ$ invites us to compare with the other diboson processes that have been considered previously. The reach is higher as expected for $\gamma\gamma \rightarrow W^+W^-$ where the signal interferes with the much larger tree-level background [6]. While a strategy of exploiting the decay products might favor the ZZ final state with respect to the W^+W^- final state, it will not be enough to overcome the different level of background. Of course, for high enough energies the signals become comparable in size and the size of the backgrounds becomes irrelevant. The reach in M_X is also slightly higher in $\gamma\gamma \rightarrow \gamma\gamma$ where contributions to the signal occur in the t and u channels as well as the s channel. This larger signal in $\gamma\gamma \rightarrow \gamma\gamma$ wins out against the larger level of standard model background in $\gamma\gamma \rightarrow ZZ$. In any

event, all of these channels should be studied to determine the universality of the graviton couplings and to test whether the signal behaves as one expects from the exchange of a spin-two particle.

V. CONCLUSIONS

The processes $\gamma\gamma \rightarrow VV$ where $VV = ZZ$ or W^+W^- are interesting reactions to look for any effects of low scale gravity. Unlike photon-photon scattering, $\gamma\gamma \rightarrow \gamma\gamma$, these cross sections occur only via s-channel exchange of gravitons. Because of the spin-two nature of the exchanged quanta, this results in nonzero matrix elements only when the initial photons have opposite helicities. Exploiting the ability of Compton backscattering to provide a hard spectrum of polarized photons, one can hope to isolate a signal.

We can suggest an overall strategy for analyzing all of the modes $\gamma\gamma \rightarrow VV$. Signals should be seen in all of the modes $\gamma\gamma \rightarrow ZZ$, $\gamma\gamma \rightarrow \gamma\gamma$, and $\gamma\gamma \rightarrow W^+W^-$ but should be absent in $\gamma\gamma \rightarrow \gamma Z$. The modes that occur only in the s channel, namely $\gamma\gamma \rightarrow ZZ$ and $\gamma\gamma \rightarrow W^+W^-$, should show a strong dependence on the polarization settings of the photon-photon collider since only the opposite helicity photons contribute to the signal. In particular the polarization setting $(P_{e_1}, P_{\gamma_1}, P_{e_2}, P_{\gamma_2}) = (+, -, -, +)$ will enhance the signal by simultaneously resulting in opposite sign backscattered photon helicities and a peak in the photon-photon luminosity at the highest energies. The signal-to-background ratio S/B for the photon-photon scattering process $\gamma\gamma \rightarrow \gamma\gamma$ should be less sensitive to the polarization setting. In this latter setting the polarizations to $(P_{e_1}, P_{\gamma_1}, P_{e_2}, P_{\gamma_2}) = (+, -, +, -)$ will enhance the sensitivity since the same photon helicity cross sections are larger than the opposite helicity cross sections.

If a graviton exchange is ever seen, then the angular dependences can be studied in detail. The rapid rise in the signal cross section means that even modest enhancements in the photon-photon collider energy can yield dramatic improvements in the rates.

ACKNOWLEDGMENTS

[1] N. Arkani-Hamed, S. Dimopoulos, and G. R. Dvali, Phys. Lett. B **429**, 263 (1998).
[2] I. Antoniadis, N. Arkani-Hamed, S. Dimopoulos, and G. R. Dvali, Phys. Lett. B **436**, 257 (1998).
[3] K. M. Cheung, Phys. Rev. D **61**, 015005 (2000).
[4] H. Davoudiasl, Phys. Rev. D **60**, 084022 (1999).
[5] S. R. Choudhury, A. Cornell, and G. C. Joshi, Phys. Lett. B **481**, 45 (2000).
[6] T. G. Rizzo, Phys. Rev. D **60**, 115010 (1999).
[7] G. Jikia, Nucl. Phys. **B405**, 24 (1993).
[8] M. S. Berger, Phys. Rev. D **48**, 5121 (1993).
[9] S. R. Choudhury, A. S. Cornell, and G. C. Joshi, Phys. Lett.

B **535**, 289 (2002).

[10] B. Bajc, Phys. Rev. D **48**, R1907 (1993).

[11] D. A. Dicus and C. Kao, Phys. Rev. D **49**, 1265 (1994).

[12] G. J. Gounaris, J. Layssac, P. I. Porfyriadis, and F. M. Renard, Eur. Phys. J. C **13**, 79 (2000).

[13] E. W. N. Glover and J. J. van der Bij, Nucl. Phys. **B321**, 561 (1989).

[14] S. Cullen, M. Perelstein, and M. E. Peskin, Phys. Rev. D **62**, 055012 (2000).

[15] I. F. Ginzburg, G. L. Kotkin, V. G. Serbo, and V. I. Telnov, Nucl. Instrum. Methods Phys. Res. **205**, 47 (1983).

[16] I. F. Ginzburg, G. L. Kotkin, S. L. Panfil, V. G. Serbo, and V. I. Telnov, Nucl. Instrum. Methods Phys. Res., Sect. A **219**, 5 (1984).

[17] V. I. Telnov, Nucl. Instrum. Methods Phys. Res., Sect. A **294**, 72 (1990).

[18] J. A. M. Vermaseren, math-ph/0010025.

[19] J. L. Hewett, Phys. Rev. Lett. **82**, 4765 (1999).

[20] P. Mathews, S. Raychaudhuri, and K. Sridhar, Phys. Lett. B **450**, 343 (1999); T. G. Rizzo, Phys. Rev. D **59**, 115010 (1999); P. Mathews, S. Raychaudhuri, and K. Sridhar, J. High Energy Phys. 07 (2000) 008; G. Shiu, R. Shrock, and S. H. H. Tye, Phys. Lett. B **458**, 274 (1999); K. M. Cheung, Phys. Lett. B **460**, 383 (1999); D. Bourilkov, J. High Energy Phys. 08 (1999) 006; K. M. Cheung and G. Landsberg, Phys. Rev. D **62**, 076003 (2000).

[21] D. Atwood, S. Bar-Shalom, and A. Soni, Phys. Rev. D **61**, 054003 (2000).

[22] K. Agashe and N. G. Deshpande, Phys. Lett. B **456**, 60 (1999); C. Balazs, H. J. He, W. W. Repko, C. P. Yuan, and D. A. Dicus, Phys. Rev. Lett. **83**, 2112 (1999); O. J. P. Eboli, T. Han, M. B. Magro, and P. G. Mercadante, Phys. Rev. D **61**, 094007 (2000); S. Mele and E. Sanchez, Phys. Rev. D **61**, 117901 (2000); K. Y. Lee, H. S. Song, and J. H. Song, Phys. Lett. B **464**, 82 (1999).

[23] T. G. Rizzo, Phys. Rev. D **60**, 075001 (1999); X. G. He, Phys. Rev. D **60**, 115017 (1999).

[24] E. Dvergsnes, P. Osland, and N. Ozturk, Phys. Rev. D **67**, 074003 (2003); N. G. Deshpande and D. K. Ghosh, Phys. Rev. D **67**, 113006 (2003).

[25] T. Gleisberg, F. Krauss, K. T. Matchev, A. Schalicke, S. Schumann, and G. Soff, J. High Energy Phys. 09 (2003) 001.

[26] C. D. Hoyle, D. J. Kapner, B. R. Heckel, E. G. Adelberger, J. H. Gundlach, U. Schmidt, and H. E. Swanson, Phys. Rev. D **70**, 042004 (2004).

[27] S. Cullen and M. Perelstein, Phys. Rev. Lett. **83**, 268 (1999).

[28] L. J. Hall and D. R. Smith, Phys. Rev. D **60**, 085008 (1999).

[29] S. Hannestad and G. G. Raffelt, Phys. Rev. D **67**, 125008 (2003); **69**, 029901(E) (2004).

[30] T. Han, J. D. Lykken, and R. J. Zhang, Phys. Rev. D **59**, 105006 (1999).

[31] G. F. Giudice, R. Rattazzi, and J. D. Wells, Nucl. Phys. **B544**, 3 (1999).

[32] M. S. Berger, C. Kao, and B. Zerbe (unpublished).

[33] G. Jikia and A. Tkabladze, Phys. Lett. B **323**, 453 (1994).